



Novel Approach to Develop an Efficient Boost Converter by Using Coupled Inductors

Mohsin Saeed, Gong Renxi, Muhammad Aurangzeb, Nadeem Asghar

Abstract—This paper focuses on the new approach to develop an efficient Boost Converter by using coupled inductors. In order to eliminate voltage spikes, a buffer circuit is used in the converter. Coupling coils generate leakage flux, and energy in the leakage flux causes voltage spikes. With a high boost ratio, the active switches in the converter can maintain the proper duty cycle, which can significantly reduce voltage and current stress. Since the main switch and the auxiliary switch can be turned on by the zero voltage switching, the switching loss is reduced, and the conversion efficiency is significantly improved. In this paper, an experiment was conducted by building a 200W boost converter model. The results show that the conversion efficiency is greater than 90%, and the surge phenomenon can be effectively suppressed. Finally, the feasibility of low-voltage input systems was verified by photovoltaic and battery system.

Keywords— Low-input-voltage, Boost Converter, Coupled Inductor, applications, Photovoltaic System.

I. INTRODUCTION (HEADING 1)

To achieve a high step-up voltage ratio, transformer- and coupled-inductor-based converters are usually the right choices. Compared with an isolation transformer, a coupled inductor has a simpler winding structure, lower conduction loss, and continuous conduction current at the primary winding, resulting in a smaller primary winding current ripple and lower input filtering capacitance. Thus, a coupled-inductor-based converter is relatively attractive because the converter. Present slow current stress and low component count. This paper introduces the new approach to develop an efficient Boost Converter by using coupled inductors [1],[5].

Photovoltaic systems (PV system) use solar panels to convert sunlight into electricity [8]. A system is made up of one or more photovoltaic (PV) panels, a DC/AC power converter (also known as an inverter) [3], a tracking system that holds the solar panels, electrical interconnections, and mounting for other components. Optionally it may include a

maximum power point tracker (MPPT), battery system and charger, solar tracker, energy management software, solar concentrators or other equipment. A small PV system may provide energy to a single consumer, or to an isolated device like a lamp or a weather instrument[7]. Large grid-connected PV systems can provide the energy needed by many customers. The electricity generated can be either stored, used directly (island/standalone plant), or fed into a large electricity grid powered by central generation plants (grid-connected/grid-tied plant).

II. LITERATURE AND REVIEW

A. DC-DC Convertors

In many industrial applications, it is required to convert a fixed-voltage dc source into a variable-voltage dc source. A dc-dc converter converts directly from dc to dc and is simply known as a dc converter. A dc converter can be considered as dc equivalent to an ac transformer with continuously variable turn ratio. Like transformer in AC, it can be used to step down or step up a dc voltage source.[1]

Dc converters are widely used for traction motor in electric automobiles, trolley cars, marine hoists, and forklift trucks. They provide smooth acceleration control, high efficiency, and fast dynamic response. Dc converter can be used in regenerative braking of dc motor to return energy back into the supply, and this feature results in energy saving for transportation system with frequent stop; and also are used, in dc voltage regulation[1],[3]. There are many types of DC-DC converter which is buck (step down) converter, boost (step-up) converter, buck-boost (step up- step-down) convertor[4].

For low power levels, linear regulators can provide a very high-quality output voltage. For higher power levels, switching regulators are used. Switching regulators use power electronic semiconductor switches in on and off states [2], [4]. Because there is a small power loss in those states (low voltage across a switch in the on state, zero current through a switch in the off state), switching regulators can achieve high efficiency energy conversion.

B. Functions of DC-DC Converters

The DC-DC converter has some functions. These are:

- i. Regulate the DC output voltage against line and load variations.
- ii. Convert a DC input voltage into a DC output voltage .

Mohsin Saeed: Guangxi university, China, Email: Mohsin.saeedciit@gmail.com.

Gong Renxi: Guangxi university, China, Email: rxgong@gxu.edu.cn.

Muhammad Aurangzeb: Hohai University, Nanjing China, Email: Maurangzaib42@gmail.com

Nadeem Asghar: Guangxi university, China, Email: engr.nadeem12@gmail.com

iii. Minimize the DC voltage ripple and DC output voltage below the required level [7].

iv. Protect the input source and the supplied system from electromagnetic interference.

v. Provide isolation between the input source and the load (if needed) [9].

The DC-DC converter is often considered as the heart of the power supply. Hence, it affects the total performance of the power supply system. Moreover, the converter accepts DC input voltage and produces a controlled DC output voltage.

Below is an overview of some kinds of DC-DC converters.

C. Boost dc-dc converters

The development of advance boost dc-dc converters has become urgent for clean-energy vehicle applications, because battery-based energy storage systems are required to cold start and battery recharge. However, back-up power from the battery is supplied using a boost converter, which is employed in many uninterrupted power supplies (UPS) [10], aerospace power systems and industrial applications. The dc back-up energy system normally consists of numerous typical low-voltage-type batteries[9]. Although series strings of storage batteries can provide a high voltage, slight mismatches or temperature differences cause charge imbalance if the series string is charged as a unit. a high-efficiency boost dc-dc converter with high voltage diversity is a key component of batteries connected in parallel. To achieve a high step-up voltage ratio, transformer- and coupled-inductor-based converters are usually the right choices [1],[7].

D. Operation

As shown in Fig. 1, the proposed converter consists of main switch set M1, boost diode Do, coupled inductors L1 and L2, the clamping circuit, and output filter capacitor Co. The clamping circuit is composed of auxiliary switch set M2, [7]

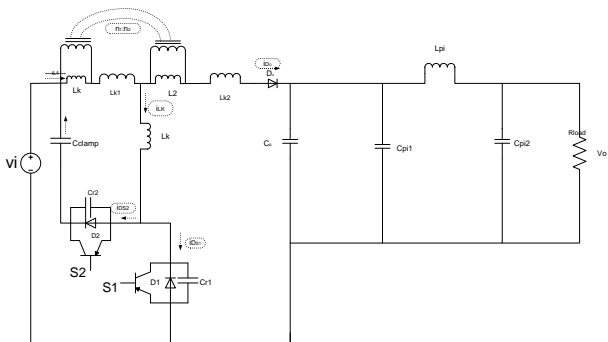
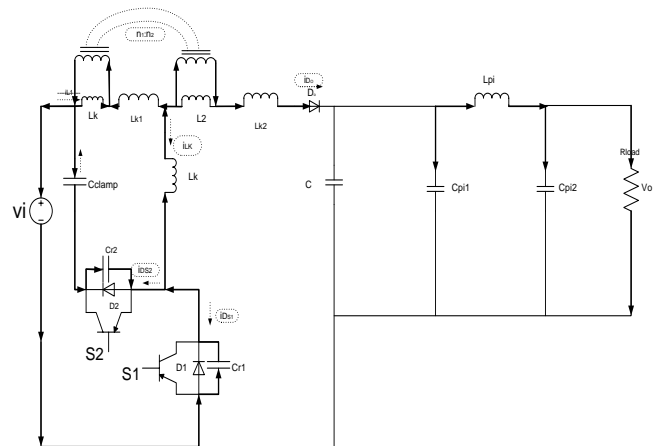


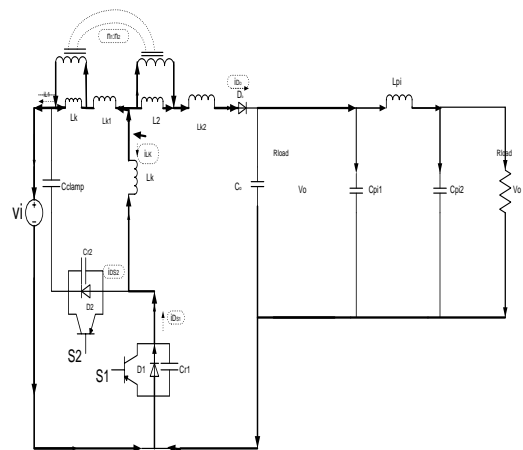
Figure 1. Proposed converter

Resonant inductor and clamping capacitor Cclamp. It should be noted that, since leakage inductor Lk1 is relatively small, inductor Lk is added to the converter to increase the load range with the ZVS condition. Switches S1 and S2 are driven in a complementary manner with a dead time to achieve ZVS. The driving signals and current and voltage waveforms of the key components are shown in Fig.1.1 shows the topological modes of the proposed converter over a switching cycle, which are explained mode by mode as follows;

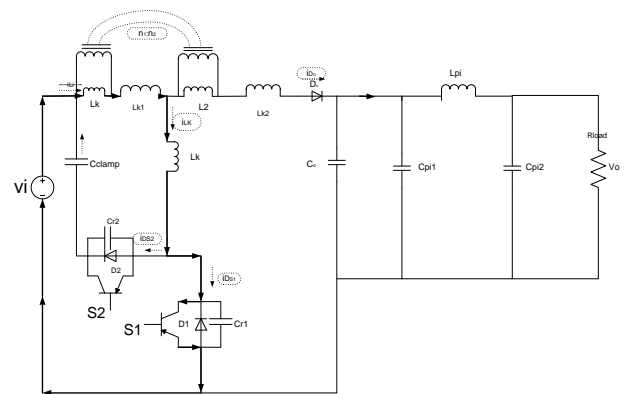
E. Topological Modes



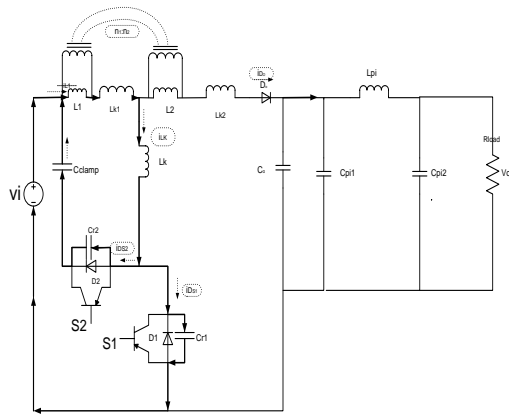
a (Mode 1)



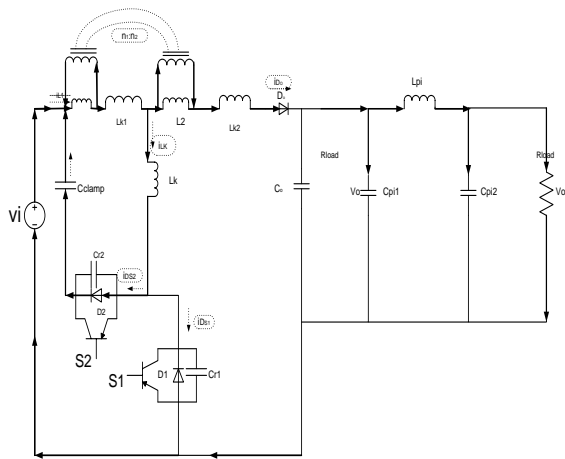
b (Mode 2)



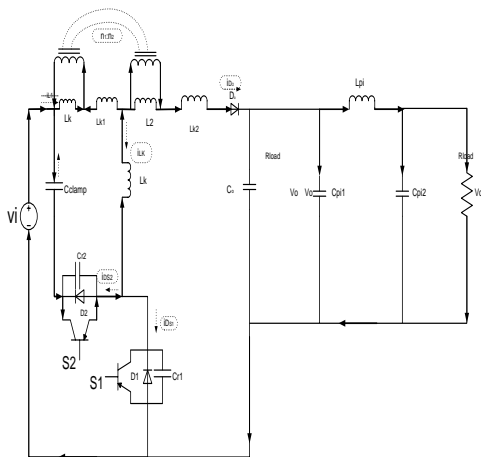
c (Mode 3)



d (Mode 4)



e (Mode 5)



f (Mode 6)

Mode 1

$[T_0 < t > T_1]$: At T_0 , auxiliary switch S2 is turned off, and main switch S1 still stays in the OFF state. In this mode, resonant inductor Lk resonates with Cr1 and Cr2, in which capacitor Cr2 is continuously charged toward $V_i + V_{clamp}$, while capacitor Cr1 is discharged down to zero. To achieve a

ZVS feature for switch S1, the energy that is stored in resonant inductor Lk should satisfy the following inequality:

$$0.5 \times [i_{Lk}(T)]^2 L_k \geq 0.5 \times [v_{DS1}(T_O)]^2 (C_{r1} \square C_{r2}) \quad (1)$$

Mode 2

$[T_1 < t > T_2]$: Mode 2 begins when voltage VDS1 drops to zero at T_1 . Inductor current i_{Lk} forces the body diode D1 of S1 to conduct and create a ZVS condition for S1. The driving signal should be applied to switch S1 when its body diode is conducting, achieving a ZVS feature. Inductor current i_{Lk} linearly increases, which can be expressed as.

$$i_{Lk}(t) = \frac{(V_i + V_o/n)}{L_k} t + i_{Lk}(T_1) \quad (2)$$

In this mode, resonant inductor current i_{Lk} increases toward zero, while diode current i_{D1} drops to zero, with its decreasing rate limited by the resonant inductor, reducing reverse recovery loss.

Mode 3

$[T_2 < t > T_3]$: This mode begins when S1 starts to conduct current at T_2 . In this mode, auxiliary switch S2 and boost diode Do are in the OFF-state, and the input current flows through the path.

Loop: . Inductor current i_{L1} is linearly increased, which can be expressed as follows:

$$i_{Lk}(t) = \frac{V_i \cdot L_1}{L_1 + L_k} \times t + i_{L1}(T_2) \quad (3)$$

Assuming .

Mode 4

$[T_3 < t > T_4]$: At T_3 , main switch S1 is turned off, while auxiliary switch S2 and boost diode Do still stay in the OFF-state. In this mode, inductors Lk and Lk1 release their energy to capacitors Cr1 and Cr2 in a resonant manner. Capacitor Cr1 is charged toward $V_i + V_{clamp}$, while capacitor Cr2 is discharged down to zero. To achieve a ZVS feature for switch S2, the energy that is stored in resonant inductor Lk should also satisfy the following inequality:

$$0.5 \times [i_{Lk}(T_3)]^2 L_k \geq 0.5 \times [v_{DS2}(T_3)]^2 (C_{r1} \square C_{r2}) \quad (4)$$

Mode 5

$[T_4 < t > T_5]$: Mode 5 begins when voltage VDS2 drops to zero at T_4 . Inductor current i_{Lk} forces the body diode D2 of S2 to conduct and create a ZVS condition for S2. The driving signal should be applied to switch S2 when its body diode is conducting, achieving a ZVS feature. In this mode, voltage VDS1 increases continuously and is clamped to $V_i + V_{clamp}$. Meanwhile, boost diode Do begins conducting. Inductor L2 is discharged through diode Do, and inductor L1 is discharged through the coupled inductors to the load. The inductor currents can be expressed as follows:

$$i_{L1}(t) = \frac{(V_o - V_i)/(1+n)}{L_1} \times t + i_{L1}(T_4) \quad (5)$$

And

$$i_{L2}(t) = \frac{(V_o - V_i)[n/(1+n)]}{L_2} \times t + i_{L2}(T_4) \quad (6)$$

Where $n = n2/n1$ is the turns ratio of the coupled inductors. The energy that is stored in resonant inductors L_k and L_{k1} is recycled to capacitor C_{clamp} . Because the capacitance of C_{clamp} is large enough, voltage V_{clamp} will remain constant. Thus, inductor current i_{Lk} is linearly decreased, which can be expressed as

$$i_{Lk}(t) = \frac{V_{clamp} - (V_o - V_i)/(1+n)}{L_k} \times t + i_{Lk}(T_4) \quad (7)$$

Mode 5 ends when inductor current i_{Lk} drops to zero.

Mode 6

$[T_5 < t < T_6]$: At T_5 , inductor current i_{Lk} reverses its direction, and capacitor C_{clamp} begins to release its stored energy through S_2 , L_k , L_{k1} , and the coupled inductors. At this interval, diode Do is conducting, and inductors L_1 and L_2 are discharged continuously to the load. When switch S_2 is turned off again at the end of mode 6, the converter operation over one switching cycle is complete.

F. Analysis

In steady-state operation of the proposed converter, time intervals ΔT_s and $(1-D)T_s$ are very short as compared to one switching period. Thus, they are not considered in the analysis of the DC voltage transfer ratio and the simplified waveforms are shown in Fig.1.1 below, in which T_s represents the switching period of the converter operation

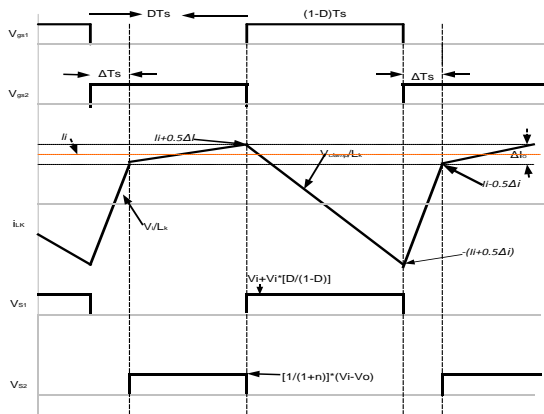


Fig 1.1 Current switching period of operation wrt time

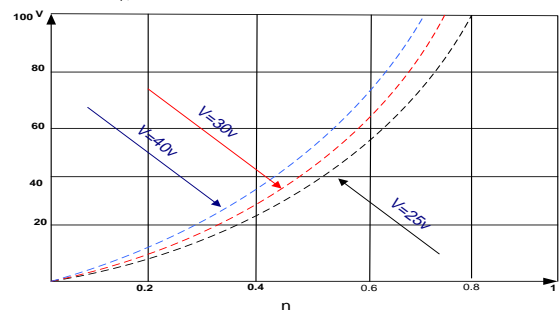


Figure 2. Relationship between voltage V_{clamp} and duty ratio

According to the plots, voltage will go beyond input voltage when D is greater than 0.5, which will result in a high voltage stress that is imposed on the components.

Thus, the duty ratio is usually limited to lower than 0.5 in the converter design. The input-to-output transfer ratio can be derived as

$$M_{ideal} = \frac{v_o}{v_i} = \frac{nD+1}{1-D} \quad (8)$$

When ignoring the charging time of resonant inductor. The charging time of the resonant inductor will reduce the effective duty ratio. The lost time interval can be expressed as

$$\Delta T_s = \frac{2I_i \times L_k}{V_i + V_o} \quad (9)$$

$$I_i = \frac{V_o I_o}{nV_i D} \quad (10)$$

And η is the conversion efficiency of the proposed converter. During the charging time, inductor L_1 is continuously discharged, and the effective duty ratio of switch S_1 will be less than that of the control signal that was applied. Thus, the input-to-output transfer ratio that is given in equation (11) should be modified to the following expression:

$$M_{real} = \frac{V_o}{V_i} = \frac{n(D - \frac{\Delta T_s}{T_s}) + 1}{1 - (D - \frac{\Delta T_s}{T_s})} \quad (11)$$

The relationships between D and for different values of turns ratio n , as illustrated in Fig 3. Comparing these two sets of curves reveals that the difference between the ideal case and the real is small for small values of D and n . From the curves that were shown in Fig. 3.

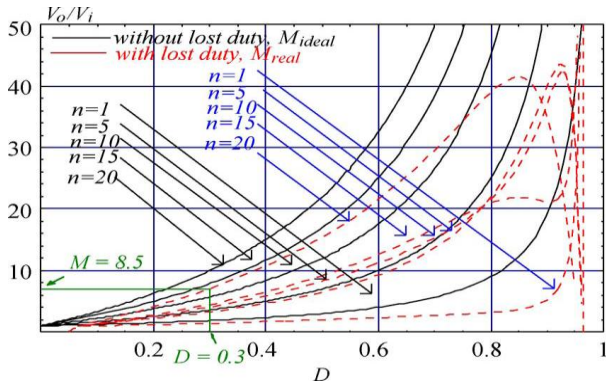


Figure 3. relationships between D and $M = V_o/V_i$

It is difficult for the converter to achieve a high step-up voltage ratio when it is operated with either a low value of n or a high value of D . Additionally the proposed converter operates in a duty ratio that is higher than 0.5, which will induce high voltage stresses on its switches.

Thus, in the design, the duty cycle is usually selected with a value that is lower than 0.5, and the turns ratio n is higher than five to achieve a high step-up voltage ratio. Analytical expressions of the component stresses are derived in the next section.

G. Current Stress and Efficiency:

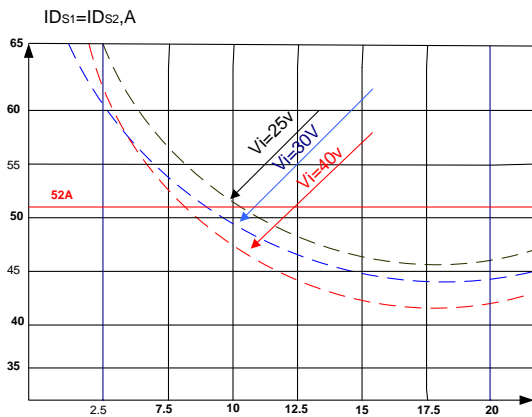


Figure 4. current stress of main switch S1 also decreases with an increase

Fig. 4 shows that the current stress of main switch also decreases with an increase in n . In the proposed converter, the voltage and current stresses of the active switches can be both reduced. Lower voltage stress implies that switches with lower can be used. Moreover, the energy that is trapped in the leakage inductance and that stored in can be recovered. It is noticeable that the stress results from voltage spike can be eliminated in the proposed converter. However, the voltage stress of the boost diode is increased with the use of coupled inductors, and high-voltage operation of a diode might induce a high reverse recovery loss. In the proposed converter, the leakage inductor of the coupled inductors can limit the decreasing rate of the diode current, resulting in lower reverse-recovery loss. In practice, selection of a high-voltage diode is easier than that of a MOSFET. Thus, it is a good tradeoff with

such a design. The key design step of the converter is to determine turns ratio n to insure low voltage stress and sufficient operational margin. In practice, the design needs a tradeoff between power losses and turns ration. For a low-input-voltage application and with soft-switching features, conduction loss will be more significant than switching loss. The conduction loss and efficiency of the proposed converter can be estimated as follows:

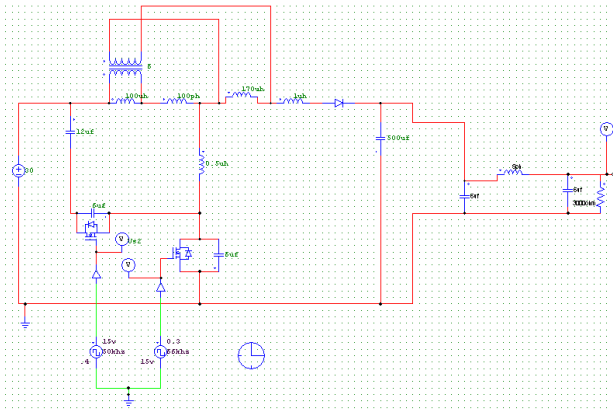
$$P_{loss} = i_{DS1}^2 r_{ds(on)} D + r_{ds(on)} (1-D) \times [(C_{r1} \square C_{r2}) v_{DS2}^2] / L_k$$

Efficiency of the converter is more than 95% on a low duty ratio. Switching loss also decreases and switching Turn-ON time is decreases to improve the efficiency of this model and decrease the losses.

III. DESIGN & SIMULATION RESULTS

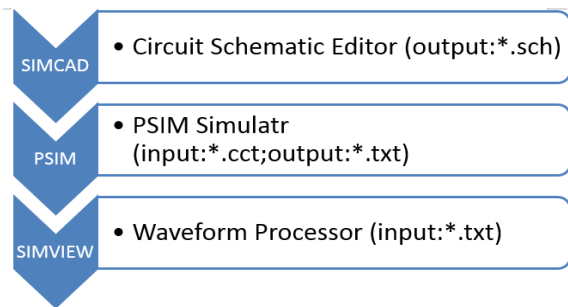
Our topological circuit is advance and efficient and is design for the following rated values which is given in table.

Input voltage (V_i)	30V
Output voltage (V_o)	411V
Voltage across switch 1 (V_{s1})	60v
Voltage across switch 2 (V_{s2})	60v
Voltage applied to switch 1 (V_{gs1})	15v
Voltage applied to switch 2 (V_{gs2})	15v
Couple inductor	$L_p=5\text{mh}; L_s=2\text{mh}; N_p=6T; N_s=38T$ EE-55 Core;
Switch	S1=S2: IRFZ44N(150v/0A) RDS (on)=0.032 Ω
Buffer	BD140
Diode	Do:Schottky diode (STPS20H100CT,500v/10A)
Capacitor	$C_o=220\mu\text{F}/1000\text{v}$ (Equivalent series resistance 3 Ω) ; $C_{clamp}=12\mu\text{F}/100\text{v}$ (Equivalent series resistance 4 Ω)

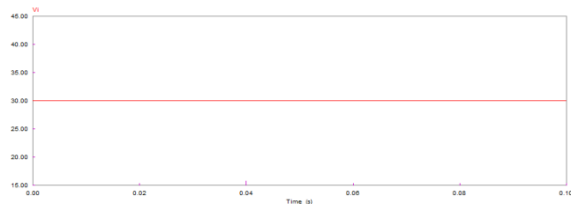


Boost converter boost the voltage from 30v to 411v approximately at this time both switches operate at 0.3 duty cycle and 66 kHz frequency. PSIM is simulation software designed for power electronics, motor control, and dynamic system simulation. The PSIM package consists of three parts: PSIM schematic program, PSIM Simulator, and waveform display program Simview.

PSIM provides an intuitive and easy-to-use graphic user interface for schematic editing. A circuit can be easily created and edited. Extensive on-line help is available for each component. To handle large systems, PSIM provides the sub circuit function which allows part of a circuit to be represented by a sub circuit block. The PSIM simulation package consists of three programs: circuit schematic editor SIMCAD, PSIM simulator, and waveform processing program SIMVIEW. The simulation environment is illustrated as follows in figure (6).

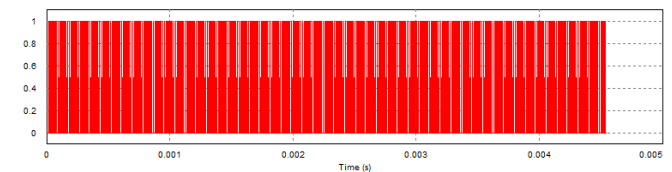
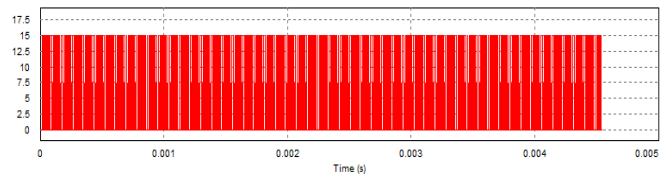


Input Voltage Wave :

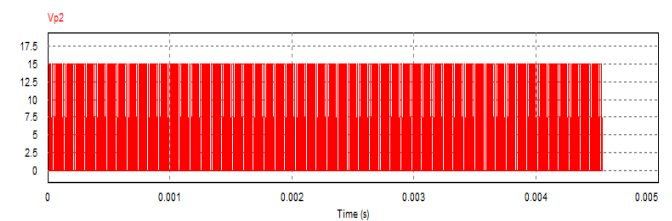


Measured waveform of the input voltage given to the proposed converter, the above figure is showing exactly a 30V input given to the circuit. X-Axis is representing a time and Y-Axis is representing a amplitude.

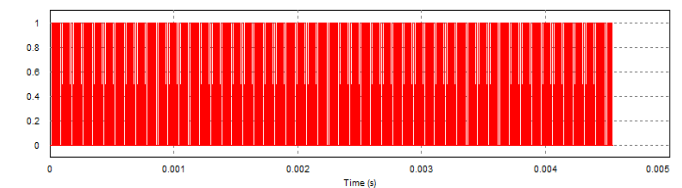
Voltage Wave Fed to Switch 1:



Measured waveform of the voltage fed at switch 1, we can see that the voltage fed to switch is exactly 15v and gate voltage also shown in the graph mentioned above. 15v is necessary to turn ON the switch.

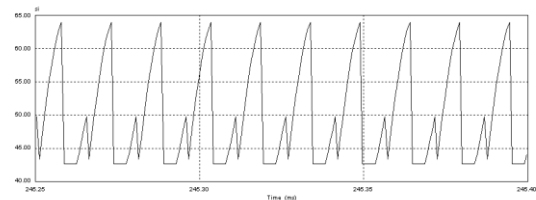


Voltage fed to switch 2



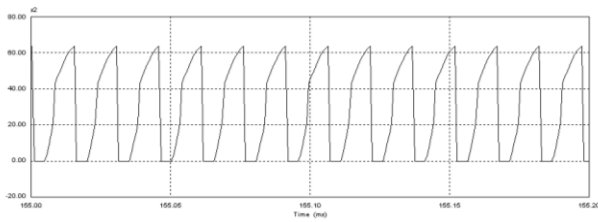
Measured waveform of the voltage fed at switch 2, we can see that the voltage fed to switch is exactly 15volts and gate voltage also shown in the graph mentioned above. 15v is necessary to turn ON the switch.

Voltage across switch 1:



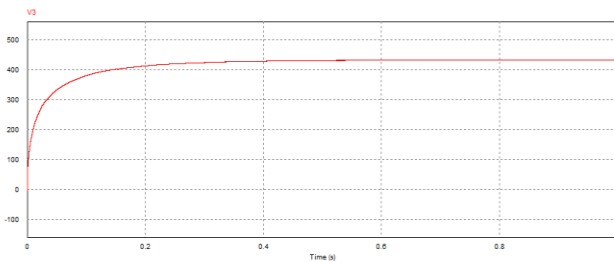
The above picture shows the voltage waveform measured across switch 1, this is voltage measured across switch one.

Voltage across switch 2:



The above picture shows the voltage waveform measured across switch 2. Above is the measured voltage as compared to the fed voltage

Output Voltage :



Measured waveform of the output voltage shows the output voltage is round about 411V.

CONCLUSION

This study developed a high-efficiency proposed boost converter with coupled inductors for power sources with large voltage diversity. The proposed converter can yield an excessive step-up voltage ratio and sustain a right duty cycle, resulting in lower electrical stresses. Through adopting the snubber circuit, the power that is trapped in the leakage inductor can be recovered, voltage spike can be suppressed efficiently and ZVS features can be accomplished successfully.

- This topology adopts only two switches to achieve the objectives of power flow.
- The voltage gain and utilization rate of the magnetic core can be substantially increased by using coupled inductors with lower turn ratio and the copper loss in magnetic core can be greatly reduced with lower turn ratio.

- The topology analysis of the converter has been provided in detail, from which layout equations and circuit parameters have also been derived. The proposed converter has an asymmetrical pulse-width-modulation system.
- Experimental results have proven that the proposed converter can gain excessive efficiency over a wide load range. It's far distinctly appropriate for low-input-voltage systems.
- Moreover, the detailed stability analysis on the control issue could be further studied by using dynamic behavior modeling techniques.

REFERENCES

- [1] O.K. Marti and H. Wino grad, Mercury Arc Rectifiers, Theory and Practice, McGraw-Hill, 1930, p.419, Fig. 221.
- [2] L. Tang G.-J. Su. An interleaved reduced-component-count multivoltage bus DC/DC converter for fuel cell powered electric vehicle applications[J]. IEEE Transactions on Industry Applications, 2008, 44(5): 1638-1644.
- [3] Irfan Jamil, Zhao Jinquan, Rehan Jamil, "Analysis, Design and Implementation of Zero-Current-Switching Resonant Converter DC-Dc Converter" International Journal of Electrical and Electronics Engineering (IJEEE), Vol. 2, Issue 2, May 2013.
- [4] O.K. Marti and H. Wino grad, Mercury Arc Rectifiers, Theory and Practice, McGraw-Hill, 1930, p.419, Fig. 221.
- [5] X. Zhang, L. Jiang, J. Deng, et al. Analysis and design of a new soft-switching boost converter with a coupled inductor[J]. IEEE Transactions on Power Electronics, 2014, 29(8): 4270-4277.
- [6] M. Aurangzeb, Z. Jinquan, I. Jamil, and M. F. Ali, "Case study of development boost converter with coupled inductors for PV system applications," in Ubiquitous Computing, Electronics & Mobile Communication Conference (UEMCON), IEEE Annual, 2016, pp. 1-6.
- [7] Zero-Voltage-Switching Boost Converter Using a Coupled Inductor Hyun-Lark Do Dept of Electronic and Information Eng., Seoul National University of Science and Technology, Seoul, Korea.
- [8] encon.fke.utm.my/courses/notes/MSc-Chopper.pdf
- [9] G. Chen, Y. S. Lee, S.Y.R. Hui, D. H. Xu, and Y. S. Wang, "Actively clamped bidirectional fly back converter," IEEE Trans. Ind. Electron, vol. 47, no. 4, pp. 770-779, Aug. 2000.
- [10] L. Schuch, C.Rech,H.L. Hey,H.A.Gründling,H.Pinheiro,and J.R.Pinheiro, "Analysis and design of a new high-efficiency bidirectional integrated ZVT PWM converter for DC-bus and battery-bank interface," IEEE Trans. Ind. Appl., vol. 42, no. 5, pp. 1321-1332, Sep./Oct.2006.